International Symposium
On Turbulence and Shear Flow
Phenomena (TSFP-8)
August 28 - 30, 2013 Poitiers, France

ANALYSIS OF THE TURBULENT FORCING IN PARTICLE-LADEN FLOW INDUCED BY RADIATION

Rémi Zamansky
Center for Turbulence Research
Stanford University
USA
remizam@stanford.edu

Filippo Coletti
Mechanical Engineering
Stanford University
USA
colettif@stanford.edu

Marc Massot
EM2C
Ecole Centrale Paris
France
marc.massot@ecp.fr

Ali Mani
Center for Turbulence Research
Stanford University
USA
alimani@stanford.edu

ABSTRACT

The proposed study focus on the interplay of hydrodynamic turbulence, radiative heating and particle transport. These three fundamental phenomena are encountered simultaneously in many branches of physical science, from meteorology to engineering, oceanography and astrophysics. The flow under interest is a novel phenomenon that is responsible for the high local concentration of inertial particles in presence of thermal radiation. Specifically, we consider a large number of particles, immersed in a transparent fluid, and subject to thermal radiation. Initial non-uniformities in particle concentration result in local temperature fluctuations, due to the different absorptivity of the dispersed and carrier phases. Under the influence of gravity or other acceleration fields, fluid motion is induced by gas expansion and buoyancy, altering the particle distribution and inducing higher non-uniformities. With respect to other dispersed multiphase flow problems, the main difference is the retroaction of the dispersed phase on the carrier fluid, which happens here through the thermal energy released in the fluid by conduction and convection. The equations of motion are simplified according to the Oberbeck-Boussinesq approximation, whereas in the particle equation of motion only the Stokes drag and the gravitational force are retained. Those equations are solved by DNS using a pseudo-spectral method, and the evolution of the particle velocities and positions is obtained by Lagrangian tracking. The objective of this paper is to investigate the consequence of the peculiar "two-way coupling" forcing and its consequences on the resulting turbulence.

INTRODUCTION

Multiphase flows in which a denser phase is carried by a lighter fluid are obliquitous in nature, and find multiple applications in industrial problems. From sandstorms in the atmosphere to plankton in the oceans, from fuel droplets in combustors to particulate emission from car exhausts, in all these cases the coupling between the dispersed and the carrier phases is critical to understand and predict the system behavior. In most relevant situations the carrier fluid flow is in the turbulent regime, and the inertial particles cannot follow its rapid fluctuations. The velocity lagging of the dispersed phase can lead to a high local concentration in zones of shear and away from vorticity cores (Squires & Eaton, 1991). If the loading is high, or the particle size is comparable to the minimal flow scales, the dispersed phase influence the carrier flow, altering for example the turbulent activity (Gore & Crowe, 1991; Boivin *et al.*, 1998; Meyer, 2012).

In several natural phenomena, turbulent dispersed multiphase flows occur under strong thermal radiation. In cloud physics, preferential concentration is believed to play an important role in determining the rate of droplet coalescence (Grabowski & Wang, 2013; Shaw, 2003). Recent direct numerical simulations show that the clustering of droplets enhances the transmittance of solar radiation (Matsuda *et al.*, 2012). In circumstellar disks, turbulent clustering appears to be critical for the aggregation of chondrules and other constituents into primitive planetesimals (Shariff, 2009; Cuzzi *et al.*, 2001). Among the many industrial applications where particle-laden turbulence presents itself in conjunction with radiation, we quote the injection of fuel sprays in combustion chambers (Watanabe *et al.*, 2008), aluminum particles in solid rocket motors (Doisneau *et al.*, 2013). Another potential application is solar energy harvesting applications, in particular solid particle solar receivers. These are direct absorption devices which use solid particles enclosed in a cavity to absorb concentrated solar radiation. Solid particles provide a high area-to-volume ratio, which enables efficient absorption of concentrated sunlight (Siegel *et al.*, 2010; Miller & Koenigsdorff, 2000; Klein *et al.*, 2007; Bertocchi *et al.*, 2004). Important is also the question of the geoengineering for climate. Solar radiation management using albedo-enhancing aerosols injected into the stratosphere has been identified as the most affordable and effective option for altering the gross radiative budget of the earth (Shepherd, 2009), but issues regarding the injection and the stability of such aerosol are still open (Keith, 2010).

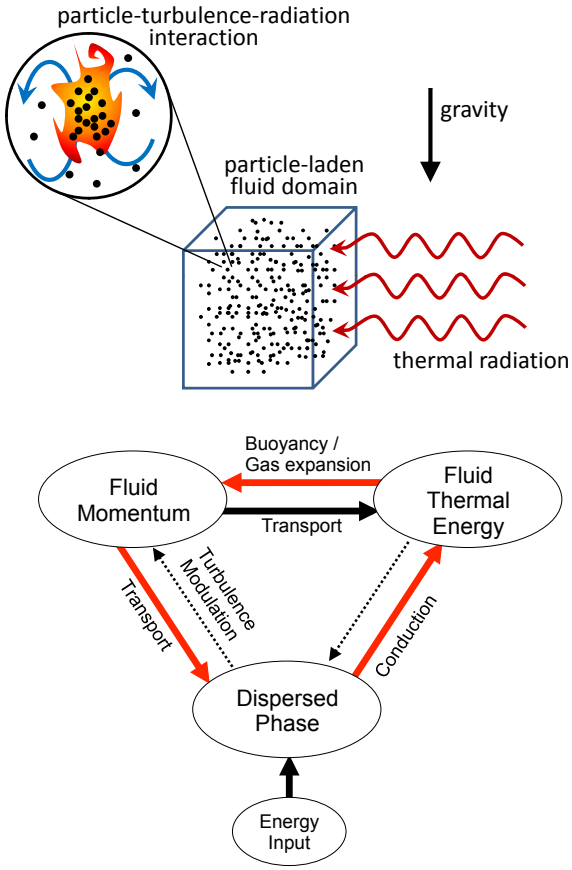

Figure 1. (a) Typical flow configuration. (b) Scheme of the interplay between fluid momentum, fluid temperature and particles. The plain arrows represent the leading order interactions. The red arrows emphasize the feedback loop.

In the proposed study the radiation provides the fundamental forcing to the fluid motion, by heating the dispersed phase providing a strong feed-back of the particles on the flow. We consider a large number of randomly distributed particles immersed in a transparent fluid (Fig. 1). Non-uniformities in particle concentration (either due to inherent randomness, or induced by previous turbulent agitation) result in local temperature variations, due to the different absorptivity of the dispersed and carrier phases. The thermal gradients lead to gas expansion and buoyancy, altering the particle distribution and potentially inducing higher non-uniformities. The relative impact of gas expansion and gravity depends on the intensity of the radiation and acceleration fields, respectively. The coupling between local particle concentration, temperature fluctuations and hydrodynamic forcing is schematically illustrated in Fig. 1. With respect to other dispersed multiphase flow problems, the main difference is the retroaction of the dispersed phase on the carrier fluid, which happens here through the thermal energy released in the fluid by conduction and convection. In this situation, the forcing of the flow is largely different from the large-scale stirring encountered in turbulent convective flows.

GOVERNING EQUATIONS

We focus on the weak radiative flux regime. In this limit, we can assume that the temperature of the system is quasi-stationary, and that the density variation is small enough to be retained only in the buoyancy forcing term. In line with these assumptions, the governing equation of the carrier phase are obtained in the framework of the Oberbeck-Boussinesq approximation with periodic boundary conditions (Borue & Orszag, 1997). They read:

$$\nabla.\mathbf{u} = 0 \tag{1}$$

$$D_t\mathbf{u} = -\frac{1}{\rho}\nabla p + \nu\nabla^2\mathbf{u} + g\alpha\theta\mathbf{e_z} \tag{2}$$

$$D_t\theta = \kappa\nabla^2\theta + \frac{q'}{\rho c_f} \tag{3}$$

where $D_t = \partial_t + \mathbf{u}.\nabla$, ν is the kinematic viscosity, κ is the thermal diffusivity, $\theta = T - \overline{T}$ is the temperature fluctuation around the reference temperature (which is take here as the spatially average fluid temperature), α is the isobaric thermal expansion coefficient, c_f is the fluid heat capacity, g is the acceleration due to the gravity, and $q' = q - \overline{q}$ represents the spatial fluctuations of the thermal source term, with $\overline{q}$ the total heat flux absorbed by the system per unit volume.

It is further assumed that the particles present a much higher density than the fluid and are very small compared to the computational mesh. It is then legitimate to consider the particles as material points. Retaining only the inertia, the drag, the gravity and the buoyancy, the evolution equations for a particle are given by:

$$d_t\mathbf{x}_p = \mathbf{u}_p \tag{4}$$

$$d_t\mathbf{u}_p = \frac{\mathbf{u} - \mathbf{u}_p}{\tau_p} + \frac{\rho_p - \rho}{\rho_p} g\mathbf{e_z} \tag{5}$$

$\mathbf{x}_p$ is the particle position coordinates, $\mathbf{u}_p$ is the particle velocity, ρ_p is the particle density, and $\tau_p = \frac{2}{9}\frac{\rho_p}{\rho}\frac{1}{\nu}\left(\frac{d}{2}\right)^2$ is the Stokes relaxation time.

Concerning the particles temperature, in order to retain only the minimal physics for capturing the dynamics of feedback loop forcing (see fig. 1), we assumed that the particles are in thermal equilibrium with the surrounding gas. This assumption correspond formally to a vanishingly small particle thermal inertia and imply that the particle temperature is equal to the fluid temperature at the particle position: $\theta_p = \theta(\mathbf{x} = \mathbf{x}_p)$.

In this flow, the only forcing comes from the thermal source term q' in Eq. (3). We assume that the carrier phase is transparent, and the incident radiative flux on each particle is totally absorbed. In addition we consider the particles as monodispersed spheres, with a number density low enough to neglect their mutual interactions, (both at short scales (collision) and long scales (screening effect)). Therefore, the thermal source term in Eq. (3) is only dependent of the relative local particle concentration:

$$q' = \sum_p \Phi_p \delta(\mathbf{x} - \mathbf{x}_p) - \overline{q} \tag{6}$$

where δ is the Dirac distribution and Φ_p represent the radiative heat flux received by one particle, and it can be related to $\overline{q}$: $\overline{q} = \Phi_p \overline{n}$ with $\overline{n}$ the particle mean number density ($\overline{n} = N_p/H^3$, H being the size of the computational domain and N_p the number of particle in this box).

Note that in Zamansky *et al.* (2013), the set of governing equations has been derived accounting for finite particle thermal inertia and it has been numerically observed that the effect of non-equilibrium between the particle and the gas temperature is negligible as long as the particle inertia is small.

CHARACTERISTIC SCALES AND NON-DIMENSIONAL EQUATIONS

Since the forcing of the flow is related to the particle segregation, we would expect the key parameter to be the particle Stokes number *i.e.* the ratio of the particle response time to the time scale of the flow structures Eaton & Fessler (1994). However, unlike in "one-way-coupled" particle-laden flows (where the fluid flow is not influenced by the dispersed phase), here the flow time scale is not known a priori. Nevertheless, an expression for the flow time scale, t_*, is derived by dimensional analysis. The size of the box, H, is assumed to be not directly relevant for the particle segregation, and τ_p is not retained in order to build a non-dimensional parameter corresponding to the Stokes number. Dimensional analysis yields $t_* = (\alpha g \beta)^{-2/5} \nu^{1/5}$ where $\beta = \dfrac{d\overline{T}}{dt} = \dfrac{\overline{q}}{\rho c_f}$ is the mean rate of fluid temperature increase. The temperature scale is set by imposing $\theta_* = \beta t_*$, and the length scale, obtained from the Brunt-Väisälä frequency $t_*^{-1} = (\alpha g \theta_*/\ell_*)^{1/2}$, is $\ell_* = (\alpha g \beta)^{-1/5} \nu^{3/5}$. Note that for consistency with the Boussinesq approximation, one should have $\overline{T}/\beta \ll t_*$, ie. the rate of increase of the mean temperature should be much smaller than the time scale of dynamics of the system.

In connection with equations (1)-(6), the non-dimensional form of the set of parameters can be expressed as: the Stokes number $St = \tau_p/t_*$, the Reynolds number (or a confinement parameters) $\gamma = H/\ell_*$, the density ratios ρ_p/ρ_f, the Prandtl number $Pr = \nu/\kappa$, the Froude number $Fr = \left(g t_*^2/\ell_*\right)^{-1/2}$ and the non-dimensional particle number density $C = \overline{n}\ell_*^3$. The non-dimensionnalization of Eq. (1)-(6) by scales θ_*, t_*, l_* and $u_* = l_*/t_*$ gives

$$\nabla.\mathbf{u} = 0 \tag{7}$$

$$D_t\mathbf{u} = -\nabla p + \nabla^2\mathbf{u} + \theta\mathbf{e_z} \tag{8}$$

$$D_t\theta = \frac{1}{Pr}\nabla^2\theta + c' \tag{9}$$

$$d_t\mathbf{x}_p = \mathbf{u}_p \tag{10}$$

$$d_t\mathbf{u}_p = \frac{\mathbf{u}-\mathbf{u}_p}{St} + \frac{\mathbf{e_z}}{Fr^2}\,. \tag{11}$$

The thermal source term c' in Eq. (9) reads:

$$c' = \sum_p^{N_p} (\delta(\mathbf{x}-\mathbf{x}_p)/\overline{n}) - 1\,. \tag{12}$$

NUMERICAL SIMULATIONS

Equations (7)-(9) are solved using a pseudo-spectral method (Canuto *et al.*, 1988) in a periodic cubic domain of length 2π. The $2/3$ rule is used for the de-aliasing of the non-linear term. The time integration is done by the second order Adams-Bashforth method.

For the particle phase, we use the Lagrangian tracking approach to compute the evolution of the particle velocities and position. The gas velocity at the particle position is estimated from cubic spline interpolation (Garg *et al.*, 2007). The time advancement for the particle equations also uses the second order Adams-Bashforth algorithm, with the same time step as the flow.

The source term (12) is a Dirac distribution which needs to be projected onto the mesh. A local particle concentration field is obtain by regularization of the Dirac masses. Following Maxey *et al.* (1997) we choose to use a Gaussian shape regularization. This reads

$$\delta(\mathbf{x}-\mathbf{x}_p) \rightarrow \delta_\sigma(\mathbf{x}-\mathbf{x}_p) = A\,\exp\left(-\frac{(\mathbf{x}-\mathbf{x}_p)^2}{\sigma^2}\right)\,, \tag{13}$$

with A a normalization parameters. The regularization length σ is choose to be commensurate to the smallest physical scale of the flow, i.e. $\sigma \approx \eta$, where the viscous scale of the flow can be estimated from the Kolmogorov relation, and is therefore independent of the mesh size $\Delta x = H/N$ (N^3 being the resolution).

The Gaussian kernel (13) is truncated for numerically efficient computations. The normalization parameter A is given by $A^{-1} = \int\int\int_{-k_2\sigma}^{+k_2\sigma} \exp\left(-(\mathbf{x}-\mathbf{x}_p)^2/\sigma^2\right) d\mathbf{x}$. In the present simulations we have chosen $k_1 = \sigma/\ell_* = 0.5$ and $k_2 = 3$ from comparison with other projection schemes (Garg *et al.*, 2007).

We have run a set of simulations for 7 Stokes numbers (ranging from $3\times\ 10^{-3}$ to 30) and 3 Reynolds numbers ($\gamma = 40,\ 80,\ 220$), keeping all other parameters constant. In particular, we imposed $1/Fr = 0$ (non-settling particles), $C = 0.35$, $Pr = 1$ and $\rho_p/\rho_f = 909$. Although gravity is necessary to generate buoyancy, non-settling particles were considered in this set of calculations in order to minimize the number of concomitant effects at play. Nevertheless, as a matter of fact, gravitational settling is found to be of influence only for $Fr < 1$ (Zamansky *et al.*, 2013).

These simulations correspond to $N_p = 2.31\cdot10^4$, $1.10\cdot10^5$ and $2.00\cdot10^6$ particles, respectively, in a domain of size $(2\pi)^3$ with computational mesh of 65^3, 128^3 and 256^3 elements, respectively. This ensure that all the physical scale of the flow are properly resolved. All simulations were initiated in quiescent conditions (zero velocity and temperature fluctuations) and particles randomly distributed in space.

RESULTS AND DISCUSSION

In the investigated regime it appears that a feedback loop between the local particle concentration, the temperature fluctuations and the buoyancy forcing can create and sustain turbulence. This is illustrated in figures 2, the temporal evolution of the turbulent kinetic energy in the box is presented for three different Stokes number ($St = 0.07$, 0.3 and 7.3). The influence of the particle response time on the dynamics is clearly seen. In all three cases, it is seen that after an initial spin up, the system reach a statistical steady-state. At low Stokes number the system presents a low level of turbulent kinetic energy and low fluctuations

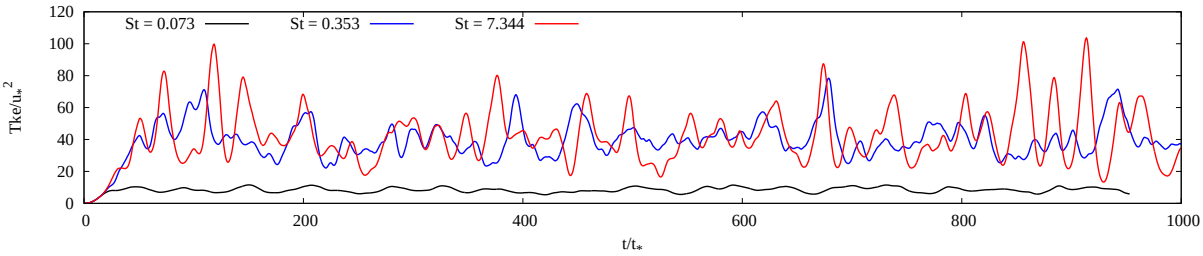

Figure 2. Time evolution of the turbulent kinetic energy for $St = 0.07$, 0.3 and 7.3, $\gamma = 80$ and $C = 0.35$.

thereof, while for higher Stokes number the turbulent kinetic energy rises and oscillates dramatically over time.

Figure 3 presents snapshots of the fluid temperature and particle local concentration in the domain, for $St = 0.07$ and 0.3, both having $\gamma = 80$ and $C = 0.35$. In the former case the fields are fairly homogeneous, whereas in the latter bulges of high temperature (the plumes) appear in correspondence with regions of high particle concentration (the clusters). The accretion and disaggregation of the clusters is entangled with the formation, merging and expansion of the hot plumes that surround them. The phenomenon is heavily intermittent, and drives large spatio-temporal fluctuations.

In Figure 4, we plot the variance of the fluid temperature and the mean turbulent kinetic energy (from both spatial and temporal average) versus the Stokes number, for three different size of the computational domain. The non-monotonic dependence of the variance of the fluid temperature as well as the turbulent kinetic energy of the system reveals the significant nonlinearity of the underlying dynamics governing this problem. In particular the peak observed around $St \approx 1$ is connected to a much higher intermittence in the particle distribution and flow structures, as seen in Fig. 3.

As a measure of the local particle concentration, in Figure 5, we plot the probability density functions of the cell volumes obtained from the Voronoï tessellation of the particle position (Monchaux *et al.*, 2010). The PDFs are compared to the case of particles being spatially distributed as in a random Poisson process (Ferenc & Néda, 2007). For both high and low Stokes number ($St = 0.003$, 0.019 and 29.36), the distributions are close to the Poisson case, which means that the particles are nearly homogeneously distributed. At intermediate Stokes numbers ($St = 0.074$, 0.352, 1.064, 7.343), the Voronoï volume distribution becomes much broader. This is the signature of intense particle clustering: there are regions without particle commensurate with the box size as well as an increase of the probability of finding particles within a very small distance.

As seen in Eq. (6), the source term in the fluid temperature equation is directly dependent of the particle distribution. Therefore the large clustering observed in Fig. 3 and 5 for $St = O(1)$ results in large temperature fluctuations (as seen in Fig 4a). The production of turbulent kinetic energy comes from the work done by the buoyancy force ($\mathscr{P} = w\theta$) and is largely influenced by the large temperature fluctuations. The Figure 6 presents the PDF of the kinetic energy production term for the different Stokes and Reynolds numbers. It is seen that at the smallest Stokes numbers the Production presents only small fluctuations commensurate with $u_*\theta_*$, while for $St \approx 1$, the PDF presents giant fluctuations with values exceeding 50 times $u_*\theta_*$ (which is of the order of the standard deviation). The skewness of the PDF is

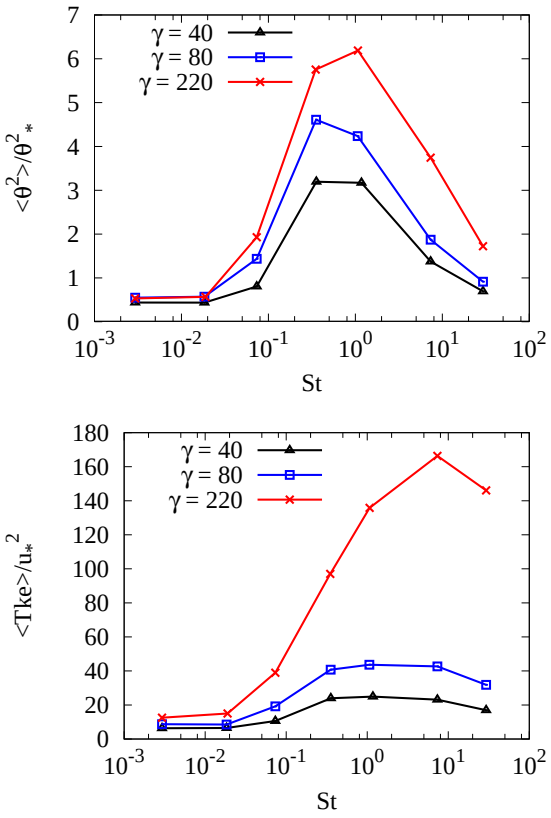

Figure 4. Evolution with the Stokes number and the St and γ of the fluid temperature variance (a) and the turbulent kinetic energy (b). For $C = 0.35$ and $\gamma = 40$, 80, 220.

due to mean positive flux of particle in the vertical direction which create a dissymmetry in the w-θ correlation (unlike homogenous turbulent convection (Calzavarini *et al.*, 2006; Borue & Orszag, 1997)).

The broadband forcing observed for $St = 0(1)$ in Fig. 6 is likely to spans the whole range a flow length scales, and alter the classical turbulence spectrum. This is observed in Figure 7, where the three-dimensional turbulent kinetic energy spectra for the different Stokes and Reynolds numbers are shown. At small stokes the spectra at large scale present departure from the classical $k^{-5/3}$ Kolmogorov spectrum. At these Stokes numbers the particle distribution is nearly homogenous (as seen in Fig. 3 and 5) and all the particles moves approximatively at the same velocity, therefore the resulting temperature fluctuations have a length scale of the order of the mean inter-particle distance leading to forcing only active at small scale. At the highest Stokes numbers, the particle have of a ballistic like motion owing to their

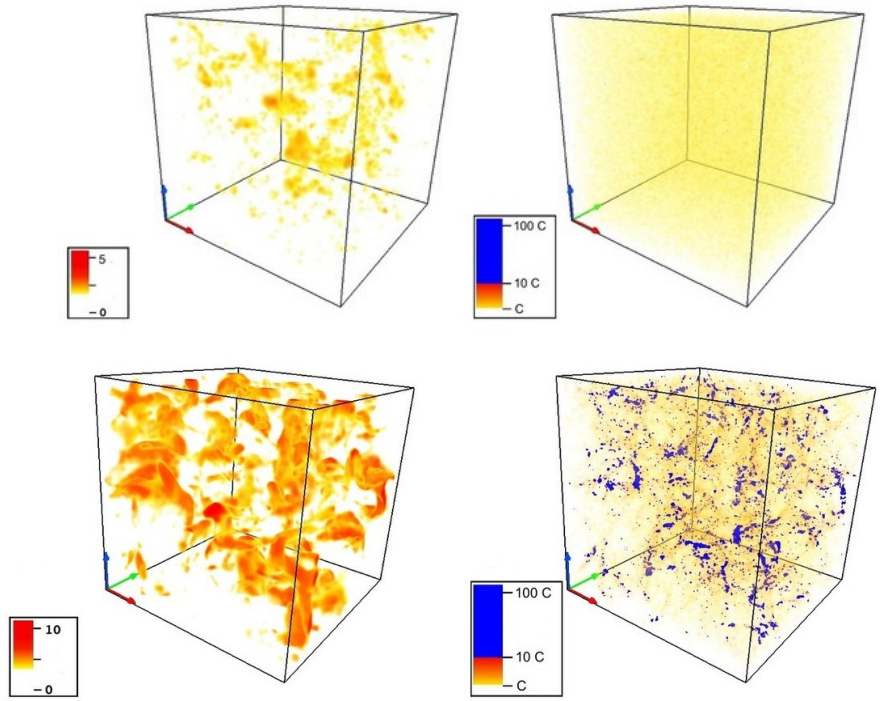

Figure 3. (a) and (b): snapshot for $\gamma = 80$ and $St = 0.07$ of the positive temperature fluctuation (colored by θ/θ_*) and particle concentration (colored by c'/C), respectively. (c) and (d): idem (a) and (b) for $\gamma = 80$ and $St = 0.3$.

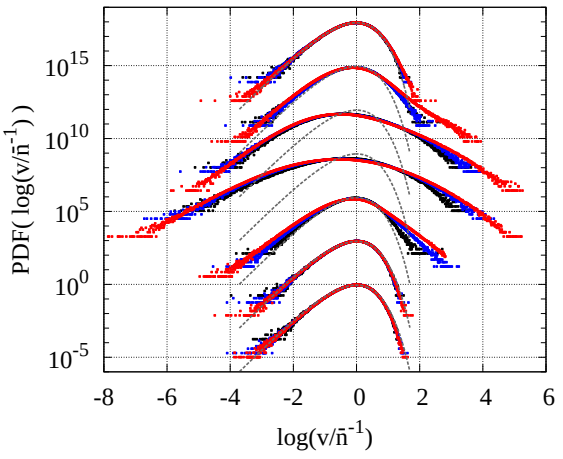

Figure 5. PDF of the logarithm of the normalized volume of the Voronoï cell, for $St = 0.003$, 0.019, 0.074, 0.352, 1.064, 7.343 and 29.36 (respectively shifted upward by 1000 units), for $\gamma = 40$ (black), 80 (blue) and 220 (red), and for $C = 0.35$. Each PDF are compared with the PDF (in gray) corresponding to the Poisson distribution.

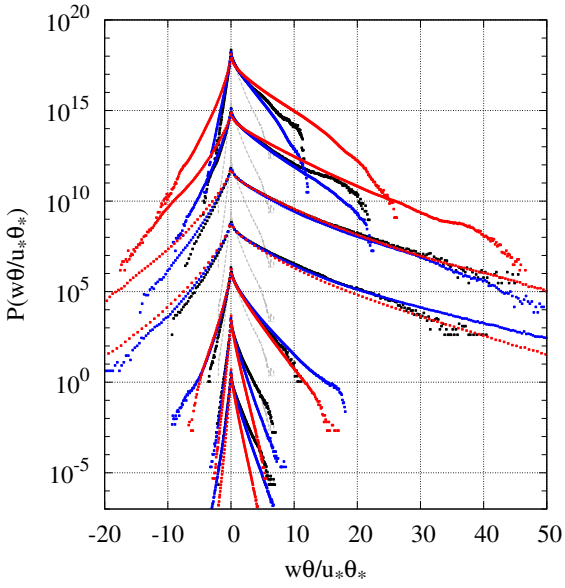

Figure 6. PDF of the turbulent kinetic energy production term $\mathscr{P} = w\theta$, for $St = 0.003$, 0.019, 0.074, 0.352, 1.064, 7.343 and 29.36 (respectively shifted upward by 1000 units), for $\gamma = 40$ (black), 80 (blue) and 220 (red), and for $C = 0.35$. Each PDF are compared with the PDF (in gray) corresponding to $St = 0.003$ and $\gamma = 40$.

large inertia, it results in large scale temperature fluctuations leading to the observed $k^{-5/3}$ spectra, although the particle are also nearly homogenously distributed (see Fig. 5). For Stokes number of order 1, we observed a very large clustering behavior of the particles, with cluster aggregation and recombination, therefore the energy input take place on a large range of time and length scale of the particle clusters altering the inertial range of the flow and leading to a k^{-1} energy spectrum.

REFERENCES

Bertocchi, R., Karni, J. & Kribus, A. 2004 Experimental evaluation of a non-isothermal high temperature solar particle receiver,. *Energy* **29**, 687–700.

Boivin, M., Simonin, O. & Squires, K. D. 1998 Direct nu-

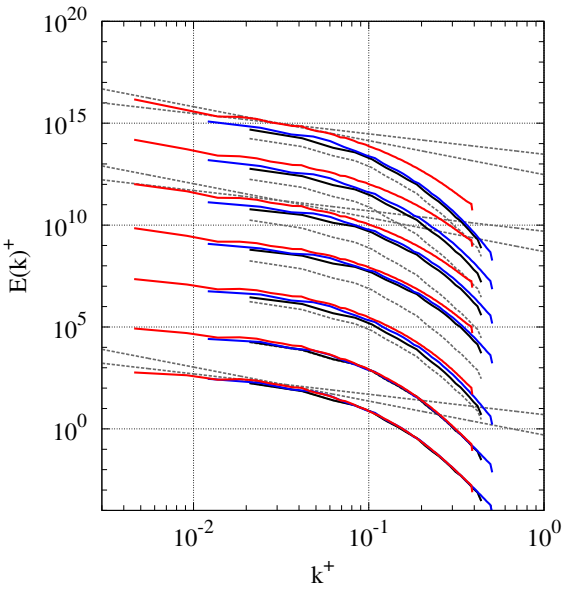

Figure 7. Three-dimensional turbulent kinetic energy spectra, for $St = 0.003$, 0.019, 0.074, 0.352, 1.064, 7.343 and 29.36 (respectively shifted upward by 1000 units), for $\gamma = 40$ (black), 80 (blue) and 220 (red), and for $C = 0.35$. Spectra are compared with the spectra corresponding to $St = 0.003$ and $\gamma = 40$ and with k^{-1} and $k^{-5/3}$ power laws.

merical simulation of turbulence modulation by particles in isotropic turbulence. *Journal of Fluid Mechanics* **375**, 235–263.

Borue, Vadim & Orszag, Steven A. 1997 Turbulent convection driven by a constant temperature gradient. *Journal of Scientific computing* **12** (3).

Calzavarini, E., Doering, C. R., Gibbon, J. D., Lohse, D., Tanabe, A. & Toschi, F. 2006 Exponentially growing solutions in homogeneous rayleigh-bénard convection. *Physical Review E* **73**, 035301.

Canuto, C., Hussaini, M.Y., Quarteroni, A. & Zang, T.A. 1988 *Spectral Methods in Fluid Dynamics*. New York: Springer-Verlag.

Cuzzi, J. N., Hogan, R. C., Paque, J.M. & Dobrovolskis, A.R. 2001 Self-selective concentration of chondrules and other small particles in protoplanetary nebula turbulence. *Astrophys. J.* **546**, 496–508.

Doisneau, F., Laurent, F., Murrone, A., Dupays, J. & Massot, M. 2013 Eulerian multi-fluid models for the simulation of dynamics and coalescence of particles in solid propellant combustion. *Journal of Computational Physics* **234**, 230 – 262.

Eaton, J. K. & Fessler, J. R. 1994 Preferential concentration of particles by turbulence. *International Journal of Multiphase Flow* **20**, 169–209.

Ferenc, J.-S. & Néda, Z. 2007 On the size distribution of poisson voronoi cells. *Physica A: Statistical Mechanics and its Applications* **385**, 518.

Garg, R., Narayanan, C. Lakehal, D. & Subramaniam, S. 2007 Accurate numerical estimation of interphase momentum transfer in lagrangian–eulerian simulations of dispersed two-phase flows. *International Journal of Multiphase Flow* **33**, 1337–1364.

Gore, R. A. & Crowe, C. T. 1991 Modulation of turbulence by a dispersed phase. *Journal of Fluids Engineering* **113** (2), 304–307.

Grabowski, Wojciech W. & Wang, Lian-Ping 2013 Growth of cloud droplets in a turbulent environment. *Annual Review of Fluid Mechanics* **45** (1).

Keith, David W. 2010 Photophoretic levitation of engineered aerosols for geoengineering. *Proc. Nat. Acad. Sc. USA* **107** (38), 16428–16431.

Klein, H. H., Karni, J., Zvi, R.B. & Bertocchi, R. 2007 Heat transfer in a directly irradiated solar receiver/reactor for solid-gas reactions. *Solar Energy* **81**, 1227–1239.

Matsuda, K., Onishi, R., Kurose, R. & Komori, S. 2012 Turbulence effect on cloud radiation. *Physical Review Letter* **108**, 224502.

Maxey, M.R., Patel, B.K., Chang, E.J. & Wang, L.P 1997 Simulations of dispersed turbulent multiphase flow. *Fluid Dynamics Research* **20** (143-156).

Meyer, Daniel W. 2012 Modelling of turbulence modulation in particle- or droplet-laden flows. *Journal of Fluid Mechanics* **706**, 251–273.

Miller, F. & Koenigsdorff, R. 2000 Thermal modeling of a small-particle solar central receiver. *J. of Solar Energy Engng.* **122**, 23–33.

Monchaux, R., Bourgoin, M. & Cartellier, A. 2010 Preferential concentration of heavy particles: a Voronoi analysis. *Physics of Fluids* **22**, 103304.

Shariff, Karim 2009 Fluid Mechanics in Disks Around Young Stars. *Annual Review of Fluid Mechanics* **41**, 283–315.

Shaw, R. 2003 Particle-turbulence interactions in atmospheric clouds. *Annual Review of Fluid Mechanics* **35**, 183–227.

Shepherd, J. et al., Royal Society Policy Document 10/09 2009 *Geoengineering the climate: science, governance and uncertainty*. London, UK: Royal Society.

Siegel, N. P., Ho, C. K. & Kolb, G. J. 2010 Development and evaluation of a prototype solid particle receiver: On-sun testing and model validation. *J. of Solar Energy Engng.* **132**, 021008.

Squires, K. D. & Eaton, J. K. 1991 Preferential concentration of particles by turbulence. *Physics of Fluids A: Fluid Dynamics* **3** (5), 1169–1178.

Watanabe, Hiroaki, Kurose, Ryoichi, Komori, Satoru & Pitsch, Heinz 2008 Effects of radiation on spray flame characteristics and soot formation. *Combustion and Flame* **152** (1-2), 2 – 13.

Zamansky, Rémi, Coletti, Filippo, Massot, Marc & Mani, Ali 2013 Particle-laden buoyant flow subject to radiation. In *International Conference on Multiphase Flow 2013 (ICMF2013)*, , vol. accepted. May 26 - 31, 2013 Jeju, Korea.